Localization Analysis of Nonlocal Models with Damage-Dependent Nonlocal Interaction

Milan Jirásek, Rodrigue Desmorat

Localization Analysis of Nonlocal Models with Damage-Dependent Nonlocal Interaction

Milan Jirásek[a,*], Rodrigue Desmorat[b]

[a] *Czech Technical University in Prague, Faculty of Civil Engineering, Department of Mechanics, Thákurova 7, 16629 Prague 6, Czech Republic, milan.jirasek@fsv.cvut.cz*
[b] *LMT, ENS Paris-Saclay/CNRS/Université Paris-Saclay, 61 avenue du Président Wilson, F-94235 Cachan Cedex, France, desmorat@lmt.ens-cachan.fr*

Abstract

This paper systematically compares and evaluates (in the one-dimensional setting) the performance of a new type of integral nonlocal averaging scheme, initially motivated by the idea of internal time that reflects the reduction of the elastic wave speed in a damaged material. The formulation dealing with internal time is replaced by the equivalent concept of a modified spatial metric leading to a damage-dependent interaction distance. This modification has a favorable effect on the evolution of the active part of damage zone and leads to its gradual shrinking, which naturally describes the transition from a thin process zone to a fully localized crack. However, when a pure damage model (with no permanent strain) is considered, the resulting load-displacement diagrams exhibit dramatic snapbacks and excessively brittle behavior in the final stages of failure. The concept of damage-dependent interaction distances is therefore extended to damage-plastic models and damage models with inelastic (permanent) strain. It is shown that, for formulations that consider a part of the strain as irreversible, the overall stress-displacement response becomes realistic for quasi-brittle materials such as concrete, for which the diagram typically exhibits a long tail.

*Corresponding author

1. Introduction

Integral-type nonlocal formulations of material models with stress softening are usually based on weighted spatial averaging with a fixed weight function that depends on the standard geometric distance between interacting material points [42, 6]. Such formulations, physically motivated [3, 4, 5, 45, 32], act as efficient localization limiters and provide an objective description of strain localization. They lead to proper convergence of numerical solutions to meaningful limits characterized by finite energy dissipation [43]. However, they also suffer by certain deficiencies, as pointed out in [12, 30, 1, 32, 7, 22, 27].

One problematic aspect is that, physically, material points located on the opposite sides of a stress-free crack should not interact even if their geometric distance is small. This natural requirement can be taken into account for a pre-existing crack (or notch), e.g., by defining the interaction distance based on the shortest path that does not cross the crack (such as in the visibility check method [10, 9]). However, such an adjustment captures only pre-existing cracks and does not reflect the effects of a growing process zone that eventually develops into a new stress-free segment. Another deficiency of the standard averaging techniques is that, when applied to models with damage driven by the nonlocal equivalent strain, they lead to a spurious expansion of the damage profile at late stages of the failure process [8]. Nonlocal (or gradient/phase field) damage models with an evolving internal length were introduced by a number of authors [20, 21, 2, 45, 39, 44, 16, 41, 49]. They could potentially be useful for modeling of a progressive transition from diffuse damage to strain localization by bridging Continuum Damage Mechanics and Fracture Mechanics, reflecting the natural expectation that the nonlocal interactions get weaker (up to vanishing) when the internal length decreases.

The objective of this paper is to systematically compare and evaluate the performance of a new type of nonlocal averaging [18], initially motivated by the idea of internal time that reflects the reduction of the elastic wave speed in a damaged material [15, 17]. Instead of internal time, one can equivalently

consider a modified spatial metric leading, in a uniformly damaged body, to a damage-dependent interaction distance (or effective distance) locally defined as the standard geometric distance divided by the square root (in terms of principal values) of the integrity tensor. In the one-dimensional (1D) non-uniform case, the effective distance $\tilde{r}(x_1, x_2) = \tilde{r}(x_2, x_1)$ between two points of abscissa x_1 and x_2 is defined by [15]

$$\tilde{r}(x_1, x_2) = \int_{\eta=\min(x_1,x_2)}^{\max(x_1,x_2)} \frac{\mathrm{d}\eta}{\sqrt{1 - D(\eta)}}, \tag{1}$$

where D is the damage variable. Previous studies indicated that this approach leads to a nice shrinking of the active part of damage zone, which naturally describes the transition to a fully localized crack [18, 47]. However, the resulting load-displacement diagrams exhibit dramatic snapbacks and excessively brittle behavior in the final stages of failure.

A known feature of concrete, not modelled in the so-called pure Damage Models, is that it exhibits permanent strains [51, 37, 36, 46], caused partially by imperfect crack closure and by dissipative processes related to crack friction. A first modeling framework is the theory of plasticity, coupled with damage in the so-called Damage-Plastic Models in the same way as in [24, 19, 38, 13, 40, 25]. A second modeling possibility is to follow Hermann and Kestin [29] and to model permanent strains as caused by damage (either isotropic [11] or anisotropic [28, 14, 33], see also [35]) in constitutive models with damage-driven inelastic strain.

In the present contribution, the concept of damage-dependent interaction distances is extended from pure damage models (DM) to damage-plastic models (DPM) and damage models with inelastic (permanent) strain (DMIS). It is shown that, for formulations that consider a part of the strain as irreversible, the overall response (including the post-peak branch) becomes realistic for quasi-brittle materials such as concrete. Furthermore, if the damage evolution laws are properly adjusted, reasonable shapes of load-displacement diagrams with a long tail can be obtained for the damage-plastic model as well, and for pure damage models the snapback behavior can be eliminated. A systematic comparison

of the basic properties of various formulations in the one-dimensional setting provides guidelines that can be followed for extensions to multiple dimensions.

2. Local Models—Basic Equations

2.1. Common Framework

Nonlocal averaging with damage-dependent interaction distance is in general applicable to any type of continuum damage model, but for the present purpose it is sufficient to restrict attention to isotropic models with a single scalar damage variable D. Such models use the stress-strain law in the form [34]

$$\boldsymbol{\sigma} = (1 - D)\mathbf{E} : \boldsymbol{\varepsilon} \tag{2}$$

where $\boldsymbol{\sigma}$ is the stress tensor, $\boldsymbol{\varepsilon}$ is the strain tensor, and $\mathbf{E}$ is the elastic stiffness tensor. The damage variable D grows from 0 for the initially intact material to 1 for the fully damaged material and its growth is usually driven by a suitably defined scalar measure of strain called the equivalent strain. In the present paper, only one-dimensional tensile response is considered, and so (2) simplifies to

$$\sigma = (1 - D)E\varepsilon \tag{3}$$

where σ is the axial stress, ε is the axial strain, and E is Young's modulus. The equivalent strain is then equal to the axial strain. Under monotonic tensile loading, the damage variable can be directly linked to the (equivalent) strain by a certain non-decreasing function g. The simplest form of the damage law is thus

$$D = g(\varepsilon) \tag{4}$$

The specific form of damage function g can be derived from the uniaxial stress-strain diagram. For instance, to obtain a stress-strain diagram with linear elasticity up to the peak stress f_t, followed by exponential softening, one needs to set

$$g(\varepsilon) = \begin{cases} 0 & \text{for } \varepsilon \leq \varepsilon_0 \\ 1 - \dfrac{\varepsilon_0}{\varepsilon} \exp\left(-\dfrac{\varepsilon - \varepsilon_0}{\varepsilon_f - \varepsilon_0}\right) & \text{for } \varepsilon > \varepsilon_0 \end{cases} \tag{5}$$

where $\varepsilon_0 = f_t/E$ is the limit elastic strain and ε_f is a parameter that controls the steepness of the softening branch.

In previous studies it was found that, for a pure damage model with a local damage law that corresponds to exponential softening, the enhancement by a nonlocal formulation with interaction distance proportional to $1/\sqrt{1-D}$ (by equation (1))leads to an excessively brittle global response, especially at late stages of the localization process [18]. One of the main objectives of the present paper is to determine which particular models enhanced by the nonlocal formulation with damage-dependent interaction distance would lead to a global response characterized by load-displacement diagrams with a relatively long tail, which is typically found in experiments for concrete and similar quasi-brittle materials.

It can be expected that the global response is affected not only by the local damage law but also by the nature of the underlying model. For instance, if the model is enriched by inelastic strains, damage evolution is slowed down and this might have a favorable effect on the shape of the load-displacement diagram. Therefore, in our comparative study, we consider the uniaxial stress-strain law in a more general form

$$\sigma = (1-D)E(\varepsilon - \varepsilon_p) \tag{6}$$

where ε_p is the inelastic (or plastic) strain. To describe the evolution of damage in a general case (not restricted to monotonic loading), a simple dependence of damage on strain is replaced by Kuhn-Tucker loading-unloading conditions

$$f_d(\kappa_d, \ldots) \leq 0, \qquad \dot{\kappa}_d \geq 0, \qquad f_d(\kappa_d, \ldots)\,\dot{\kappa}_d = 0 \tag{7}$$

in which κ_d is the damage-driving variable, f_d is the damage loading function (which depends not only on κ_d but also on additional variables, to be specified later), and the superimposed dot denotes the time derivative. The specific definition of f_d and κ_d depends on the considered type of model.

2.2. Damage Model (DM)

For a pure damage model, no inelastic strain is considered, and the damage variable is driven by the maximum previously reached strain level. This model

fits into the general framework (6)–(7) if we set

$$f_d(\kappa_d, \varepsilon) = \varepsilon - \kappa_d \tag{8}$$

$$D = g_d(\kappa_d) \tag{9}$$

$$\varepsilon_p = 0 \tag{10}$$

Function g_d controls the shape of the local stress-strain curve and directly corresponds to the function previously denoted as g; see Eq. (4).

2.3. Damage-Plastic Model (DPM)

A popular family of damage-plastic models is based on a yield function written in terms of the effective stress and on damage driven by the cumulative plastic strain. Loading-unloading conditions corresponding to the plastic part of the model read

$$f_p(\ldots, \kappa_p) \leq 0, \qquad \dot{\kappa}_p \geq 0, \qquad f_p(\ldots, \kappa_p)\, \dot{\kappa}_p = 0 \tag{11}$$

where f_p is the yield function, and κ_p is the cumulative plastic strain. In the present one-dimensional context with tensile yielding only, the yield function can be defined as

$$f_p(\tilde{\sigma}, \kappa_p) = \tilde{\sigma} - \sigma_Y(\kappa_p) \tag{12}$$

where [34]

$$\tilde{\sigma} = \frac{\sigma}{1 - D} = E(\varepsilon - \varepsilon_p) \tag{13}$$

is the effective stress and σ_Y is a function that describes the dependence of the current yield stress on the cumulative plastic strain (isotropic hardening).

In the present simple case (yielding under uniaxial tension), there is no difference between the plastic strain and the cumulative plastic strain, which is formally described by the rate equation

$$\dot{\varepsilon}_p = \dot{\kappa}_p \tag{14}$$

with the initial values of both ε_p and κ_p set to zero. The cumulative plastic strain at the same time plays the role of the damage-driving variable, and so we

set

$$f_d(\kappa_d, \varepsilon_p) = \varepsilon_p - \kappa_d \tag{15}$$

$$D = g_{dp}(\kappa_d) \tag{16}$$

The shape of the stress-strain diagram is affected by functions σ_Y and g_{dp}.

2.4. Model With Damage-Driven Inelastic Strain (DMIS)

In contrast to the previous model with damage driven by plastic strain, here we use the opposite approach. A pure damage model with damage driven by the total strain is enhanced by inelastic strain that depends on the damage variable [29, 11, 28, 33]. This is described by

$$f_d(\kappa_d, \varepsilon) = \varepsilon - \kappa_d \tag{17}$$

$$D = g_{dis}(\kappa_d) \tag{18}$$

$$\varepsilon_p = \alpha_{dis}(D) \tag{19}$$

The shape of the stress-strain diagram is affected by functions α_{dis} and g_{dis}.

2.5. Correspondence Between Local Models

For a fair evaluation of the effects of nonlocality, we need to make sure that the local response of the considered models is the same, or at least similar. The pure damage model (DM) from Section 2.2 is used as the starting point, and the other two models from Sections 2.3–2.4 are adjusted (cross-identified) so that they give the same stress-strain curve under monotonic loading.

According to the **damage model (DM)** described by (6)–(10), we get

$$\sigma = \sigma_d(\varepsilon) \equiv [1 - g_d(\varepsilon)]E\varepsilon \tag{20}$$

For a given stress-strain diagram described by function σ_d, the corresponding damage function is easily evaluated as

$$g_d(\varepsilon) = 1 - \frac{\sigma_d(\varepsilon)}{E\varepsilon} \tag{21}$$

For the **damage-plastic model (DPM)** described by (6)–(7) and (11)–(16), we first have to evaluate the dependence of the plastic strain on the total strain by solving equation

$$E(\varepsilon - \varepsilon_p) = \sigma_Y(\varepsilon_p) \tag{22}$$

which can be derived by combining (12)–(14) with the assumption of plastic yielding, characterized by $f_p = 0$. Once ε_p is known as a function of ε, we can express from (13) the effective stress

$$\tilde{\sigma}(\varepsilon) = E[\varepsilon - \varepsilon_p(\varepsilon)] \tag{23}$$

and then, from (6) combined with (16), also the nominal stress

$$\sigma = \sigma_{dp}(\varepsilon) \equiv [1 - g_{dp}(\varepsilon_p(\varepsilon))]\,\tilde{\sigma}(\varepsilon) = [1 - g_{dp}(\varepsilon_p(\varepsilon))]\,E\,[\varepsilon - \varepsilon_p(\varepsilon)] \tag{24}$$

If function σ_{dp} describing the stress-strain diagram is known, the above equations are not sufficient to identify two independent functions of the damage-plastic model, g_{dp} and σ_Y. One can first select an arbitrary function σ_Y and then determine

$$g_{dp}(\varepsilon_p) = 1 - \frac{\sigma_d(\varepsilon_p + \sigma_Y(\varepsilon_p)/E)}{\sigma_Y(\varepsilon_p)} \tag{25}$$

In this way, it is possible to construct pairs of functions g_{dp} and σ_Y that correspond to exactly the same stress-strain curve under monotonic loading but to different unloading branches.

For the **damage model with inelastic strain (DMIS)** described by equations (6)–(7) and (17)–(19), the stress under monotonic loading is expressed as

$$\sigma = \sigma_{dis}(\varepsilon) \equiv [1 - g_{dis}(\varepsilon)]\,E\,[\varepsilon - \alpha_{dis}(g_{dis}(\varepsilon))] \tag{26}$$

Again, we have two functions to determine, g_{dis} and α_{dis}. Suppose that we want to match not only the monotonic stress-strain curve but also the unloading branches of the diagram that correspond to the damage-plastic model. These requirements lead to conditions of equal stress values and equal damage values generated by both models at each strain level:

$$[1 - g_{dis}(\varepsilon)]\,E\,[\varepsilon - \alpha_{dis}(g_{dis}(\varepsilon))] = \sigma_d(\varepsilon) \tag{27}$$

$$g_{dis}(\varepsilon) = g_{dp}(\varepsilon_p(\varepsilon)) \tag{28}$$

The second condition gives directly function g_{dis}, and then from the first condition we get a formula for the composed function

$$\alpha_{dis}(g_{dis}(\varepsilon)) = \varepsilon - \frac{\sigma_d(\varepsilon)}{E[1 - g_{dis}(\varepsilon)]} \tag{29}$$

To construct an explicit formula for α_{dis}, we must invert g_{dis} and then set

$$\alpha_{dis}(D) = g^*_{dis}(D) - \frac{\sigma_d(g^*_{dis}(D))}{E(1-D)} \tag{30}$$

where g^*_{dis} denotes the inverse function of g_{dis}.

2.6. Example—Exponential Softening

To provide a specific example, consider a stress-strain diagram with linear elasticity up to the peak, followed by exponential softening. Under monotonic loading, the dependence of stress on strain is described by

$$\sigma(\varepsilon) = \begin{cases} E\varepsilon & \text{for } \varepsilon \le \varepsilon_0 \\ f_t \exp\left(-\dfrac{\varepsilon - \varepsilon_0}{\varepsilon_f - \varepsilon_0}\right) & \text{for } \varepsilon > \varepsilon_0 \end{cases} \tag{31}$$

where f_t is the tensile strength, $\varepsilon_0 = f_t/E$ is the limit elastic strain, and ε_f is a parameter that controls the steepness of the softening branch. This is the model that was used in one-dimensional examples in [18].

For the **pure damage model (DM)**, we need to get $\sigma_d(\varepsilon) = \sigma(\varepsilon)$, and so the damage function has to be set to

$$g_d(\varepsilon) = 1 - \frac{\sigma(\varepsilon)}{E\varepsilon} = \begin{cases} 0 & \text{for } \varepsilon \le \varepsilon_0 \\ 1 - \dfrac{\varepsilon_0}{\varepsilon} \exp\left(-\dfrac{\varepsilon - \varepsilon_0}{\varepsilon_f - \varepsilon_0}\right) & \text{for } \varepsilon > \varepsilon_0 \end{cases} \tag{32}$$

as already indicated in (5), where the damage function was denoted simply as g.

Since the monotonic stress-strain law does not uniquely define the models with plastic or inelastic strains, we use an additional assumption that the **damage-plastic model (DPM)** is characterized by **linear hardening of its plastic part**. The dependence of the effective yield stress on plastic strain is thus given by

$$\sigma_Y(\varepsilon_p) = f_t + H\varepsilon_p \tag{33}$$

where f_t is the initial yield stress (playing also the role of tensile strength) and $H \geq 0$ is the hardening modulus. To get the same exponential softening law (31) as for the damage model, we need to define the damage function of the damage-plastic model according to (25) as

$$g_{dp}(\varepsilon_p) = 1 - \frac{\sigma_d(\varepsilon_p + \sigma_Y(\varepsilon_p)/E)}{\sigma_Y(\varepsilon_p)} = 1 - \frac{f_t}{f_t + H\varepsilon_p} \exp\left(-\frac{(1 + H/E)\varepsilon_p}{\varepsilon_f - \varepsilon_0}\right) \quad (34)$$

For the linear hardening law (33), equation (22) has a linear form

$$E(\varepsilon - \varepsilon_p) = f_t + H\varepsilon_p \quad (35)$$

and can be solved analytically. The resulting dependence of plastic strain on total strain (during monotonic loading) is given by

$$\varepsilon_p(\varepsilon) = \frac{E\varepsilon - f_t}{E + H} \quad (36)$$

Now we can proceed to the **damage model with inelastic strain (DMIS)** and match it to the DPM model. Various versions of the DMIS model can be constructed, with the same monotonic stress-strain curve (exponential) but different rules for the slope of unloading branches. Three typical cases are analyzed in detail in Appendix A and summarized in Table 1.

Table 1: Three versions of the DMIS (and two subversions as special cases)

version	parameters	$g_{dis}(\varepsilon)$	$\alpha_{dis}(D)$
1	ε_0, ε_f, E_{ep}	$1 - \frac{1}{1 + (E_{ep}/E)(\varepsilon/\varepsilon_0 - 1)} \exp\left(-\frac{\varepsilon - \varepsilon_0}{\varepsilon_f - \varepsilon_0}\right)$	$g^*_{dis}(D) - \frac{\sigma_d(g^*_{dis}(D))}{E(1-D)}$
1s	ε_0, ε_f	$1 - \exp\left(-\frac{\varepsilon - \varepsilon_0}{\varepsilon_f - \varepsilon_0}\right)$	$-(\varepsilon_f - \varepsilon_0)\ln(1-D)$
2	α, p	implicitly given by (74)	αD^p
2s	α	$\frac{\varepsilon + \alpha - \sqrt{(\varepsilon+\alpha)^2 - 4\alpha[\varepsilon - \sigma_d(\varepsilon)/E]}}{2\alpha}$	αD
3	α	$\frac{\varepsilon - \sigma_d(\varepsilon)/E}{\varepsilon + \alpha}$	$\frac{\alpha D}{1-D}$

Version 1 is constructed such that the local stress-strain curve (including unloading) exactly matches that obtained with the DP model. Parameter H of

the DP model, which represents the plastic modulus, is transformed into the elastoplastic modulus

$$E_{ep} = \frac{EH}{E+H} \tag{37}$$

For a nonzero value of H, function g_{dis} cannot be inverted in closed form and the inverse function g^*_{dis} must be evaluated numerically. In the special case of $H = 0$, which is in Table 1 referred to as version 1s, function g_{dis} gets simpler and its inversion can be done analytically, which leads to a closed-form expression for function α_{dis}.

Instead of matching the unloading response to the DP model, one can match only the response during monotonic loading and select the specific form of function α_{dis} as needed. If this function is postulated as a power law with a general exponent p, the corresponding function g_{dis} cannot be obtained in closed form and must be computed numerically; see version 2 in Table 1. In the special case with exponent $p = 1$ (version 2s in Table 1), an analytical formula for g_{dis} can be derived. Also, for another simple form of α_{dis} given by $\alpha D/(1-D)$ (which goes to infinity when D tends to 1), the corresponding function g_{dis} can be constructed; see version 3 in Table 1. A detailed analysis of the specific forms of functions g_{dis} and α_{dis} for individual versions of the model is provided in Appendix A.

2.7. Algorithmic Treatment

For the pure damage model, the evaluation of damage and stress that correspond to a given strain increment is straightforward. For the damage-plastic model, it could be somewhat more involved in a general multiaxial case—one would need to first compute the effective stress and cumulative plastic strain using an elastoplastic stress-return algorithm and then evaluate the resulting damage and nominal stress [25, 52]. However, in the present uniaxial case, the elastoplastic stress return algorithm can be replaced by simple rules that compare the elastically evaluated trial stress with the stress value that would correspond to the current total strain under monotonic loading.

More attention needs to be paid to the damage model with inelastic strain, which can be considered in several versions that differ by the rules for unloading; see Table 1. The stress evaluation algorithm for the DMIS can be summarized as follows:

1. First, the value of κ_d is determined by updating the maximum strain reached so far.
2. The next step depends on the particular version of the model.
   (a) **Version 1, including 1s:** Based on equations (18) and (65), we compute damage and inelastic strain:

$$D = g_{dis}(\kappa_d) = 1 - \frac{1}{1 + (E_{ep}/E)(\kappa_d/\varepsilon_0 - 1)} \exp\left(-\frac{\kappa_d - \varepsilon_0}{\varepsilon_f - \varepsilon_0}\right) \tag{38}$$

$$\varepsilon_p = \beta_{dis}(\kappa_d) = \frac{E}{E + H}(\kappa_d - \varepsilon_0) \tag{39}$$

   (b) **Version 2:** Based on equation (74), with $\sigma_d(\varepsilon)$ given by (31) and $\alpha_{dis}(D)$ by (77), we compute damage iteratively as the limit of D_k given by

$$D_k = D_{k-1} - \frac{F(D_{k-1})}{F'(D_{k-1})}, \qquad k = 1, 2, \ldots \tag{40}$$

   starting from $D_0 = 0$ and checking that the iterated values remain between 0 and 1. Function F and its derivative F' are defined in (78)–(79). Then we evaluate

$$\varepsilon_p = \alpha_{dis}(D) \tag{41}$$

   (c) **Version 2s:** Based on equations (70) and (72), with $\sigma_d(\kappa_d)$ given by (31), we compute damage and inelastic strain:

$$D = g_{dis}(\kappa_d) = \frac{\kappa_d + \alpha}{2\alpha} - \sqrt{\left(\frac{\kappa_d - \alpha}{2\alpha}\right)^2 + \frac{\varepsilon_0}{\alpha} \exp\left(-\frac{\varepsilon - \varepsilon_0}{\varepsilon_f - \varepsilon_0}\right)} \tag{42}$$

$$\varepsilon_p = \alpha_{dis}(D) = \alpha D \tag{43}$$

(d) **Version 3:** Based on equation (73), with $\sigma_d(\varepsilon)$ given by (31) and $\alpha_{dis}(D)$ by (80), we compute damage and inelastic strain:

$$D = g_{dis}(\kappa_d) = \frac{\kappa_d - \sigma_d(\kappa_d)/E}{\kappa_d + \alpha} = \frac{\kappa_d}{\kappa_d + \alpha} - \frac{\varepsilon_0}{\kappa_d + \alpha} \exp\left(-\frac{\varepsilon - \varepsilon_0}{\varepsilon_f - \varepsilon_0}\right) \tag{44}$$

$$\varepsilon_p = \alpha_{dis}(D) = \alpha \frac{D}{1 - D} \tag{45}$$

3. Finally, the stress is obtained as

$$\sigma = (1 - D)E(\varepsilon - \varepsilon_p) \tag{46}$$

3. Nonlocal Formulations

3.1. Fixed Interaction Distance

In general, nonlocal formulations of the models described in Sections 2.1–2.4 can be based on weighted spatial averaging of the damage-driving variable. The standard nonlocal approach would use a fixed weight function $\alpha(x, \xi)$, defined for instance as

$$\alpha(x, \xi) = \frac{\alpha_0(|x - \xi|)}{\int_{\mathcal{L}} \alpha_0(|x - \eta|)\, \mathrm{d}\eta}, \qquad r = |x - \xi| \tag{47}$$

where $\mathcal{L}$ is the one-dimensional domain of interest, usually taken as the interval $[0, L]$ where L is the length of the analyzed bar, and α_0 is a suitable function describing the decay of nonlocal interaction effects with increasing distance r. This function can be taken for instance as

$$\alpha_0(r) = \left\langle 1 - \left(\frac{r}{R}\right)^2 \right\rangle^2 \tag{48}$$

where $\langle \ldots \rangle$ are Macauley brackets (denoting the positive part, i.e., $\langle x \rangle = \max(0, x)$), and R is a model parameter with the dimension of length, which reflects the internal length scale of the material and is referred to as the nonlocal interaction radius. Physically, R should be related to the size and spacing of major heterogeneities in the material microstructure.

For the pure damage model (DM), damage is driven by the maximum previously reached value of the equivalent strain, which, in the one-dimensional

case, equals the total strain. In displacement-based versions of the finite element method, the strain at the end of an incremental computational step is iteratively updated, and in each iteration it is treated as a given quantity. Therefore, evaluation of the nonlocal strain

$$\bar{\varepsilon}(x) = \int_{\mathcal{L}} \alpha(x,\xi)\varepsilon(\xi)\,\mathrm{d}\xi \tag{49}$$

is fully explicit. The same holds for the DMIS. In nonlocal versions of these models (DM or DMIS), equation (8) or (17) is replaced by

$$f_d(\kappa_d, \bar{\varepsilon}) = \bar{\varepsilon} - \kappa_d \tag{50}$$

The stress evaluation algorithm remains the same, just the meaning of the damage-driving variable is different. If needed, one could also use an over-nonlocal formulation, with the loading function defined as

$$f_d(\kappa_d, \bar{\varepsilon}, \varepsilon) = m\bar{\varepsilon} + (1-m)\varepsilon - \kappa_d \tag{51}$$

where m is an additional dimensionless parameter. Values $m = 0$ and $m = 1$ would correspond to the local model and standard nonlocal model, respectively. The so-called over-nonlocal formulation uses $m > 1$. It was originally proposed for nonlocal plasticity [53, 50], and later adapted to nonlocal plasticity combined with damage [26], but it is in principle applicable to damage with inelastic strain as well.

For the damage-plastic model, the damage-driving variable is the maximum previously reached value of the cumulative plastic strain. In the nonlocal version and one-dimensional setting, equation (15) is replaced by

$$f_d(\kappa_d, \bar{\varepsilon}_p) = \bar{\varepsilon}_p - \kappa_d \tag{52}$$

where

$$\bar{\varepsilon}_p(x) = \int_{\mathcal{L}} \alpha(x,\xi)\varepsilon_p(\xi)\,\mathrm{d}\xi \tag{53}$$

is the nonlocal plastic strain. In a general multiaxial setting, the nonlocal cumulative plastic strain would be used. Again, one can envision an over-nonlocal formulation [26], with

$$f_d(\kappa_d, \bar{\varepsilon}_p, \varepsilon_p) = m\bar{\varepsilon}_p + (1-m)\varepsilon_p - \kappa_d \tag{54}$$

3.2. Damage-Dependent Interaction Distance

The nonlocal formulations described in the previous subsection consider the nonlocal weight function $\alpha_0(r)$ as fixed. The strength of nonlocal interaction decays with increasing distance r between points x and ξ.

As mentioned in the Introduction, a constant internal length (here the nonlocal interaction radius R) associated with the standard definition $r = |x - \xi|$ of the interaction distance between points x and ξ provides regularization and removes pathological sensitivity to the mesh, but also leads to a spurious expansion of the damage profile at late stages of the failure process [8]. This is due to the fact that, in the averaging of the damage-driving variable, points located on the opposite sides of a highly damaged zone interact in the same manner as in the zero- or low-damage case. A new form of nonlocal integral averaging that makes a highly damaged zone (at $D \approx 1$) equivalent to a crack has been proposed in [15, 17, 16], following the idea that elastic wave propagation is slowed down by a damage field, possibly heterogeneous, in a so-called nonlocal integral formulation with an internal time instead of an internal length (see also [48], in which the non-local interactions are computed by means of thermal expansions of circular inclusions centered at each material point).

Analogy with formulations based on internal time motivates nonlocal models with interaction distance modified by damage. In 1D, the effective distance $\tilde{r}$ between points x and ξ is defined in (1), for easier reference rewritten here:

$$\tilde{r}(x,\xi) = \int_{\min(x,\xi)}^{\max(x,\xi)} \frac{\mathrm{d}\eta}{\sqrt{1 - D(\eta)}} \tag{55}$$

The effective distance is then used for evaluation of the modified nonlocal weight function

$$\alpha(x,\xi) = \frac{\alpha_0(\tilde{r}(x,\xi))}{\int_{\mathcal{L}} \alpha_0(\tilde{r}(x,\eta))\,\mathrm{d}\eta} \tag{56}$$

Evaluation of the effective distance is greatly facilitated by the fact that, in the one-dimensional space, points x and ξ are connected by one single path (straight segment) and the effective distance is obtained simply by summing the effective lengths of all infinitesimal segments into which this path is divided. In

multiple dimensions, a straight path does not always lead to the shortest effective distance, and minimization over all possible continuous paths connecting x with ξ needs to be invoked [18]: the effective distances are computed in a Riemannian space curved by damage (see [47] for 2D computations using Fast Marching methods). The associated (general) computational procedures are not studied in the present work. Here we focus on fundamental localization properties of models with damage-dependent nonlocal interaction (55), which can be assessed in one spatial dimension.

3.3. Evaluation of Effective Distance by Numerical Integration

In numerical simulations by finite elements, the integral in (55) must be approximated by a finite sum, and it is natural and convenient to use the same set of Gauss integration points that are used for the evaluation of internal forces and stiffness coefficients. Typically, linear two-node elements with one integration point per element are used.

Suppose that the Gauss points are numbered consecutively and arranged in ascending order according to their x-coordinate. In a straightforward implementation, the numerical evaluation of the effective distance between points x_i and x_j (with $j > i$) can be based on the trapezoidal rule, which leads to

$$\tilde{r}(x_i, x_j) = \int_{x_i}^{x_j} \frac{\mathrm{d}x}{\sqrt{1 - D(x)}} \approx \sum_{k=i+1}^{j} \frac{1}{2} \left(\frac{1}{\sqrt{1 - D(x_{k-1})}} + \frac{1}{\sqrt{1 - D(x_k)}} \right) (x_k - x_{k-1}) \tag{57}$$

This rule would be exact if the function $1/\sqrt{1 - D(x)}$ were linear between the neighboring Gauss points. However, if D approaches 1 at the center of the damage zone, function $1/\sqrt{1 - D(x)}$ becomes highly nonlinear and the integration error increases. Numerical results show that the distribution of damage between neighboring Gauss points is close to linear, and so it is better to approximate $D(x)$ by a linear function and perform an analytical integration. The contribution of one typical subinterval is then evaluated as

$$\int_{x_{k-1}}^{x_k} \frac{\mathrm{d}x}{\sqrt{1 - D(x)}} \approx \int_{x_{k-1}}^{x_k} \frac{\mathrm{d}x}{\sqrt{1 - D(x_{k-1}) \frac{x_k - x}{x_k - x_{k-1}} - D(x_k) \frac{x - x_{k-1}}{x_k - x_{k-1}}}} =$$

$$= \frac{2(x_k - x_{k-1})}{\sqrt{1 - D(x_{k-1})} + \sqrt{1 - D(x_k)}} \tag{58}$$

and the resulting modified distance is given by

$$\tilde{r}(x_i, x_j) = 2 \sum_{k=i+1}^{j} \frac{x_k - x_{k-1}}{\sqrt{1 - D(x_{k-1})} + \sqrt{1 - D(x_k)}} \tag{59}$$

In the next section, it will be demonstrated that numerical results obtained with this improved integration scheme are better, not only for the pure damage model (Fig. 1a), but also for the damage-plastic model (Fig. 2) and for the damage model with inelastic strain (Fig. 5).

4. Numerical Results for Models With Exponential Softening

Localization properties of nonlocal versions of the constitutive models DM, DPM and DMIS described in Section 2 will be studied via simulations of a prismatic bar fixed at its left end and subjected to an increasing displacement imposed at its right end. Body forces, inertia effects and rate dependence of the material response are neglected, which means that the equilibrium condition is reduced to the condition of uniform stress along the bar. The bar length is set to $L = 100$ mm and the sectional area is supposed to be constant along the bar (its precise value is irrelevant because all the results will be presented in terms of stresses instead of forces). The material is characterized by Young's modulus $E = 30$ GPa and uniaxial tensile strength $f_t = 3$ MPa, which corresponds to the limit elastic strain $\varepsilon_0 = f_t/E = 10^{-4}$. The local stress-strain curve under monotonic loading is supposed to be given by (31), with $\varepsilon_f = 10^{-3}$. Objectivity of the model and finite energy dissipation are enforced by a nonlocal formulation. The bell-shaped polynomial weight function (48) is used, with the radius of nonlocal interaction set to $R = 20$ mm.

The present study is focused on the evolution of the damage zone inside the specimen and on the global post-peak response. Potential localization at the boundary is suppressed by imposing symmetry of the solution with respect to the middle section of the bar. The meshes are graded such that the spatial resolution

in the expected damage zone near the middle section is sufficient. The number of elements is always odd and the axis of symmetry passes through the center of an element (not through a node of the finite element mesh). Localization is triggered by the reduction of the sectional area of the central element by 0.1%. The mesh referred to as "coarse" consists of 45 elements and the element size in the damage zone is equal to 2 mm. The mesh referred to as "medium" consists of 121 elements and the element size in the damage zone is equal to 0.95 mm. The mesh referred to as "fine" consists of 241 elements and the element size in the damage zone is equal to 0.49 mm.

4.1. Damage Model

For the pure damage model with exponential softening, one-dimensional simulations of strain localization were performed in [18], with the conclusion that the global response of the bar becomes increasingly brittle at later stages of the localization process. The computed load-displacement diagrams (here actually stress-displacement diagrams) exhibit a dramatic snapback. To capture this behavior in a stable way, the simulation is performed under indirect displacement control, with the control variable defined as the relative displacement of the nodes of the element crossing the axis of symmetry. Equivalently, one could describe the loading process as being controlled by the maximum local strain.

Despite the careful choice of the control variable, it turns out that a simulation with evaluation of the effective interaction distance based on the trapezoidal rule (57) leads to a solution which does not evolve in a continuous fashion until complete failure of the specimen. At a certain stage of the degradation process, the numerical solution (stress and total elongation of the bar) changes by a jump within one incremental step, even if the step size is prescribed as very small (see the dashed curve in Fig. 1). This jump in global response is accompanied by a sudden localization of damage increments into one single element (while before the jump the zone of growing damage spans over five or more elements). The dashed curve plotted in Fig. 1 has been obtained for the coarse mesh but the same problem arises even for finer meshes.

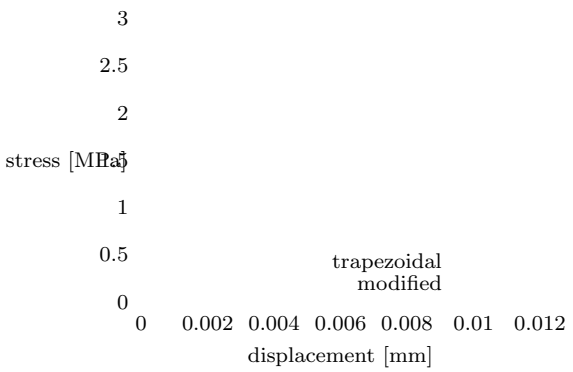

Figure 1: Influence of the integration scheme on stress-displacement diagrams for nonlocal damage model with damage-dependent nonlocal interaction: "trapezoidal" = effective distance evaluated using (57), "modified" = effective distance evaluated using (59)

A careful examination of the numerical solution reveals that the problem originates from a poor performance of the trapezoidal rule applied to the integral in (57). If the integral is evaluated using formula (59), which is better adapted to the highly nonlinear character of the integrated function for damage values close to 1, then the simulations lead to a continuous response; see the solid curve in Fig. 1. However, the diagram still exhibits snapback and the behavior at late stages of localization can be characterized as extremely brittle. This might be realistic for certain materials, but not for quasibrittle materials such as concrete, which are typically characterized by load-displacement diagrams with an initially steep descent followed by a long tail. It is therefore interesting to check whether such diagrams could be obtained for damage models that combine stiffness degradation with irreversible strains, in the form of either a damage-plastic formulation, or a damage model with inelastic strain.

4.2. Damage-Plastic Model

As the starting point, we consider a formulation based on the plastic model with linear plastic hardening described by (33), for which the dependence of plastic strain on total strain (during monotonic loading) is given by (36). The softening curve is considered as exponential, which leads to function g_{dp} defined by (34).

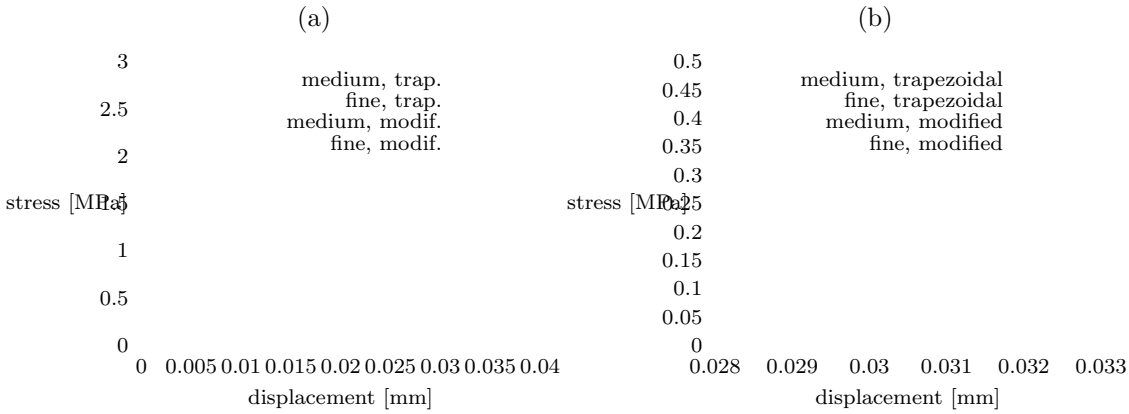

Figure 2: Influence of the element size and integration scheme on stress-displacement diagrams for DPM with parameters $H = E/30$ and $m = 2$

Localization behavior of the nonlocal version of the damage-plastic model depends on the choice of the plastic modulus H. In [26] it was shown that, in the context of a standard nonlocal formulation, $H = 0$ leads to a fully localized plastic zone. This is similar to the so-called basic nonlocal plastic model, which was analyzed, e.g., in [31]. In numerical simulations, the local plastic strain always localizes into one finite element, but the dissipation tends to a nonzero limit as the mesh is refined. The nonlocal plastic strain is nonzero in an interval of length $2R$ where R is the nonlocal interaction radius. Since the nonlocal plastic strain is the variable that drives damage, the damage variable is also nonzero in this interval. A finite size of the plastic zone is obtained if the plastic modulus H is set to a positive value, or if the damage is considered to be driven, according to (54), by the over-nonlocal plastic strain $m\bar{\varepsilon}_p + (1-m)\varepsilon_p$ with $m > 1$, or if both modifications are combined ($H > 0$ and $m > 1$).

The first simulation is performed with $H = E/30 = 1$ GPa and $m = 2$. All other parameters have the same values as in the previous case of a pure damage model, presented in Section 4.1. Nonlocal interaction weights are computed using the damage-dependent effective distance (55). The resulting stress-displacement curve plotted in Fig. 2a has a slightly concave shape and, in contrast to the curve obtained with the pure damage model (Fig. 1), does not

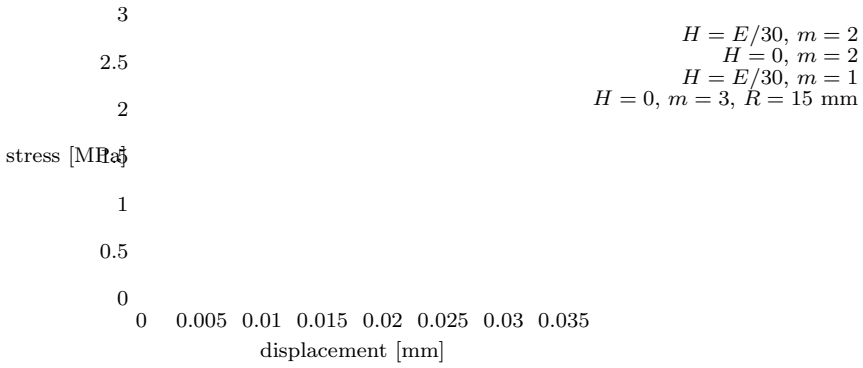

Figure 3: Stress-displacement diagrams for DPM with various combinations of parameters

exhibit a dramatic snapback. A closer examination of the terminal part of the curve reveals a slight snapback at a stage very close to complete failure, i.e., at a very low stress; see the close-up in Fig. 2b. The active part of the plastic zone gradually shrinks and the snapback occurs when the plastic strain increments become concentrated into one single element. This phenomenon is reduced if the mesh refined, and also if the damage-dependent effective distance is evaluated using the modified scheme (59) instead of the trapezoidal rule (57). The quality of results obtained with the modified rule on the medium mesh is comparable to those obtained with the trapezoidal rule on the fine mesh. As the mesh is refined, the results seem to converge to a reasonable limit curve which has no snapback.

Fig. 3 shows how the shape of the stress-displacement curve is affected by model parameters. For reference, the results obtained with $H = E/30$ and $m = 2$ are shown as the dashed curve. The solid curve corresponds to an over-nonlocal model without hardening ($H = 0$ and $m = 2$); it has a slightly convex shape with a short tail. The dotted curve corresponds to a nonlocal (not over-nonlocal) model with hardening ($m = 1$, $H = E/30$). The shape is slightly concave, quite close to a straight line. Reduction of parameter m leads to a more brittle response, with reduced area under the stress-displacement curve. On the other hand, increasing m to 3 would lead to a wider damage profile and

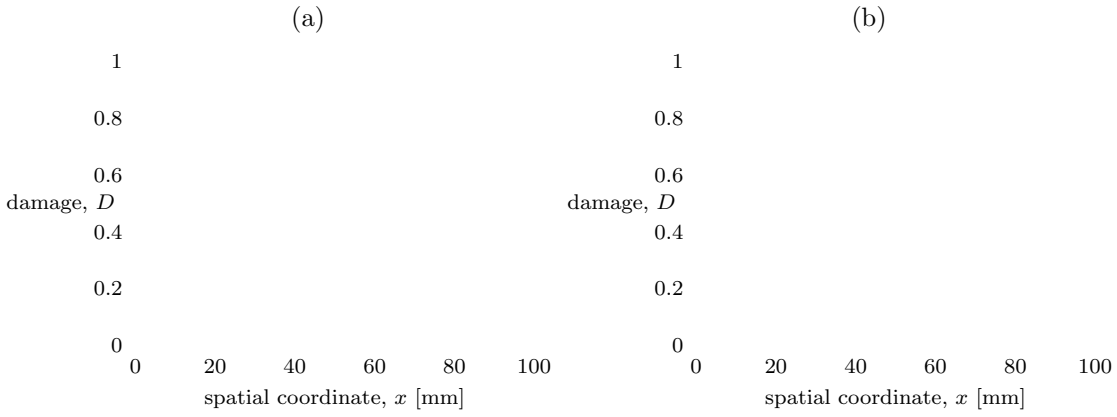

Figure 4: Evolution of the damage profiles for DPM with parameters (a) $H = 0$ and $m = 2$, (b) $H = E/30$ and $m = 1$

lower post-peak slope of the stress-displacement curve. We can compensate for that by reducing the nonlocal interaction radius R. The dash-dotted curve in Fig. 3 corresponds to an over-nonlocal formulation with $m = 3$, no hardening of the underlying plastic model ($H = 0$) and nonlocal interaction radius set to $R = 0.015$ m instead of the value $R = 0.02$ m, used in all the other simulations. The resulting shape of the stress-displacement diagram is very similar to that obtained for $m = 2$ and $R = 0.02$ m (solid curve).

As shown in Fig. 4a, the intermediate damage profiles obtained with $H = 0$ have a flat central part, but the final damage profile is nicely localized and damage tends to 1 at one section only. The flat central part of the damage profile is a characteristic feature of nonlocal damage-plastic models with no plastic hardening, as already observed in [26]. The zone of uniform damage corresponds to the active plastic zone, i.e., to the interval in which the local plastic strain is growing. In this interval, the yield condition is satisfied and, since the stress must be uniform along the whole bar (due to equilibrium), the product of the effective yield stress and the integrity factor $1 - D$ must be uniform along the active part of the plastic zone. For the formulation with a perfectly plastic model ($H = 0$) extended by damage, the effective yield stress remains equal to f_t, which leads to a uniform distribution of damage along the

active part of the plastic zone. Damage is driven by the nonlocal plastic strain, and so the zone of growing damage is larger than the plastic zone, due to the effect of nonlocal averaging. However, both zones gradually shrink and damage tends to 1 exclusively in the central cross section. A more usual shape of the damage profiles is obtained for nonlocal damage-plastic models with a positive plastic modulus ($H > 0$), irrespective of whether the formulation is standard nonlocal ($m = 1$) or over-nonlocal ($m > 1$); see Fig. 4b.

The results are encouraging—the damage-plastic model with damage-dependent nonlocal interaction provides stress-displacement curves that do not exhibit a dramatic snapback and, for the over-nonlocal damage formulation combined with a perfectly plastic backbone model, the curves can even have a slightly convex shape with a short tail, while the active part of the damage zone gradually shrinks (which would not be the case for a nonlocal damage-plastic model with fixed interaction weights).

4.3. Damage Model with Inelastic Strain (DMIS)

Let us now check whether a similar improvement of the shape of load-displacement diagrams can be achieved if the damage model is enriched by inelastic strain, as described in Section 2.4. Same as for the previously discussed models (DM and DPM), the modified integration scheme based on (59) leads to better results than the trapezoidal rule (57); see an example in Fig. 5, computed for version 2 of DMIS. Therefore, all subsequently reported results are computed using the modified scheme.

For versions 1 and 2 of the model, the stress-displacement diagrams exhibit snapback; see Fig. 6. Version 1 would give in the local 1D setting exactly the same response as the damage-plastic model introduced in Section 2.3. However, the nonlocal formulation leads to a different behavior, because the damage-plastic model evaluates damage from the nonlocal plastic strain while the DMIS evaluates plastic strain as well as damage from the nonlocal total strain. The solid curve in Fig. 6a corresponds to version 1 of DMIS derived from a damage-plastic model with no plastic hardening ($H = 0$), and the dashed curve to

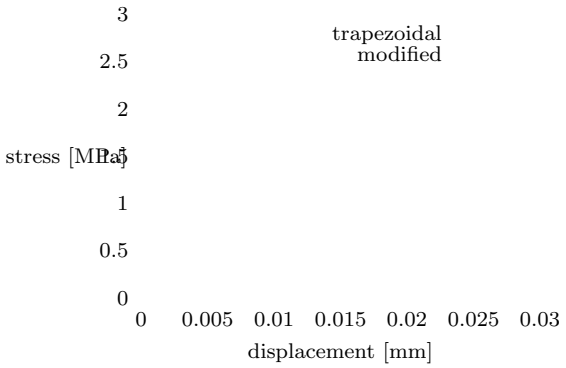

Figure 5: Influence of the integration scheme on stress-displacement diagrams for DMIS (version 2, $\alpha = 10^{-3}$, $p = 0.8$)

the DMIS derived from a damage-plastic model with linear plastic hardening ($H = E/30$). The response is continuous (thanks to the modified integration scheme) but the shape of the curves is similar to those obtained with the pure damage model, just the snapback occurs later.

The overall shape of the curve remains the same even for version 2s with inelastic strain proportional to damage; see the dashed curve in Fig. 6b. If the dependence of inelastic strain on damage is described by the power law (77), i.e., $\varepsilon_p = \alpha D^p$, with exponent p higher or smaller than 1, the shape is still the same; see the dotted and solid curves in Fig. 6b. An increase of parameter α only extends the ductile part of the curve and shifts the snapback to a later stage; see the dash-dotted curve.

Interestingly, quite an acceptable shape of the stress-displacement diagram is obtained with version 3 of the DPS model, which uses the hyperbolic law (45). Fig. 7 shows the diagrams obtained with various values of parameter α. The curves have a steep initial part followed by a very long tail. The tail is even somewhat too long, especially for the dashed curve that corresponds to $\alpha = 10^{-4}$. A reasonable load-displacement diagram was obtained with $\alpha = 0.5 \cdot 10^{-4}$; see the solid curve.

The evolution of damage, strain and plastic strain in the simulation with $\alpha = 0.5 \cdot 10^{-4}$ is plotted in Fig. 8. Plastic strains are localized in a narrow

band (Fig. 8d) while damage is more spread out (Fig. 8a). In reality, the band in which plastic strain is nonzero coincides with the band in which damage is nonzero, but the plastic strain values that correspond to moderate damage levels are very small. For instance, for $D = 0.5$ the corresponding plastic strain is equal to α, which is only $0.05 \cdot 10^{-3}$ and on the scale of Fig. 8d such strains appear to be negligible. Plastic strains exceeding $0.5 \cdot 10^{-3}$ are attained only at points where damage exceeds $10/11$. The final shape of the damage profile seems to be rounded but the band in which damage grows at late stages of the process is extremely narrow and eventually shrinks to one single integration point; see Fig. 8b (in this graph, values computed at Gauss integration points are connected by straight lines).

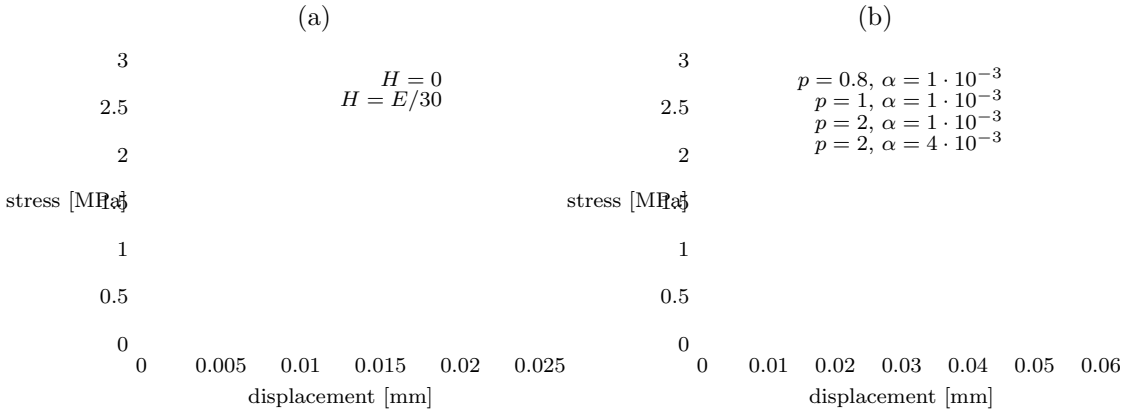

Figure 6: Stress-displacement diagrams for DMIS: (a) version 1, (b) version 2

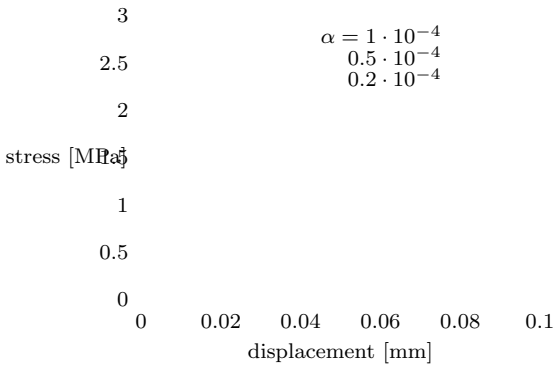

Figure 7: Stress-displacement diagrams for version 3 of DMIS

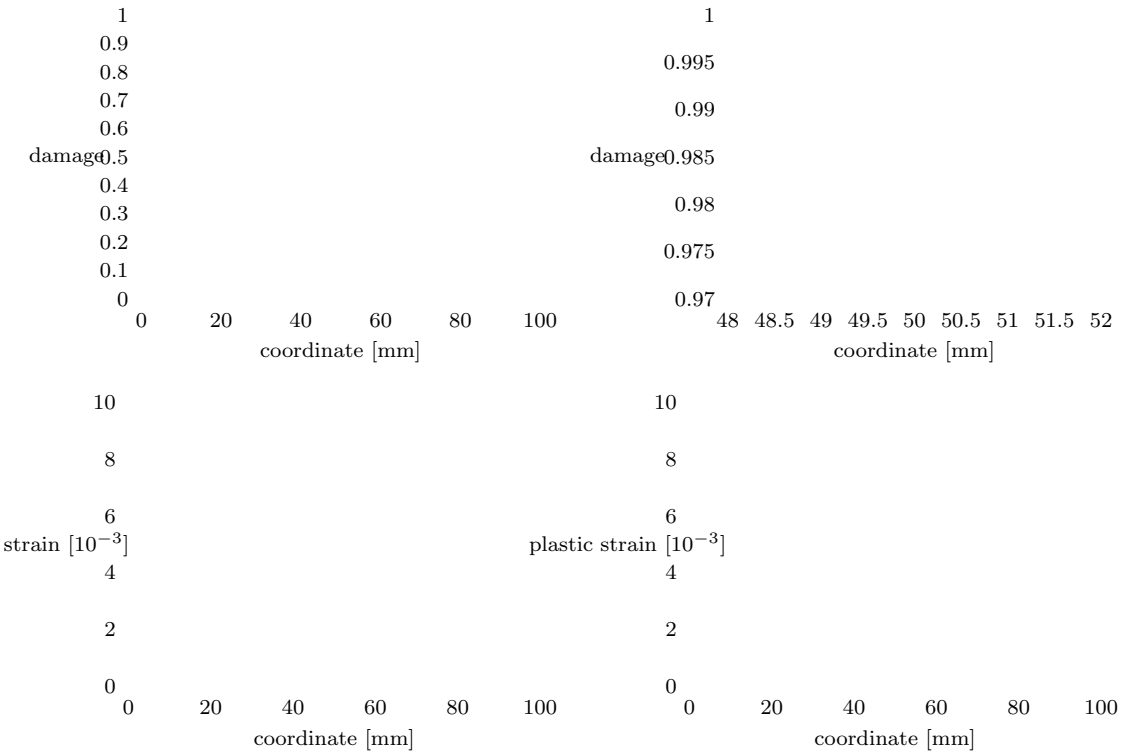

Figure 8: Version 3 of DMIS with $\alpha = 0.5 \cdot 10^{-4}$: evolution of the profiles of (a)–(b) damage, (c) total strain, (d) plastic strain

5. Damage-Plastic Model with Double-Exponential Law

So far the most promising results, presented in Section 4.2, have been obtained with the damage-plastic model and parameters $H = 0$ and $m = 2$. However, the tail of the dashed stress-displacement curve in Fig. 3 may still be considered as too short for concrete; see e.g. [23]. For $H = 0$, the damage function (34) has the form

$$g_{dp}(\varepsilon_p) = 1 - \exp(-a\varepsilon_p) \tag{60}$$

where $a = 1/(\varepsilon_f - \varepsilon_0)$, and this type of law leads to an exponential shape of the local stress-strain diagram. To extend the tail, one can first try out a modified damage function that combines two exponentials:

$$g_{dp}(\varepsilon_p) = 1 - (1 - c_2)\exp(-a\varepsilon_p) - c_2\exp(-a_2\varepsilon_p) \tag{61}$$

Here, c_2 and a_2 are two additional parameters. For $c_2 = 0$, the standard exponential law (60) is recovered. Parameters a and a_2 should be sufficiently different, just like relaxation times in viscoelasticity. The stress-displacement diagrams obtained with parameters $H = 0$ and $m = 2$ and with two sets of parameters of the double-exponential law (61) are shown in Fig. 9. The dashed curve corresponds to $a = 1000$, $a_2 = 100$ and $c_2 = 0.1$, and the solid curve to $a = 1200$, $a_2 = 120$ and $c_2 = 0.2$. For the second set of parameters, the stress-displacement curve has a very reasonable shape for concrete. The profiles of damage, plastic strain and nonlocal plastic strain obtained with these parameters are shown in Fig. 10. The damage profiles in Fig. 10a have a flat central part, for reasons explained in Section 4.2. The size of the active damage zone gradually decreases and damage tends to 1 at the central section only, as shown in Fig. 10b. The profiles of local and nonlocal plastic strain have the usual shape and are much more localized than the damage profiles; see Fig. 10c-d. On the scale of these graphs, the total strain profiles would look very similar to the (local) plastic strain profiles.

Since the approach based on the double-exponential softening law turns out to be successful for the damage-plastic model with no plastic hardening, we can

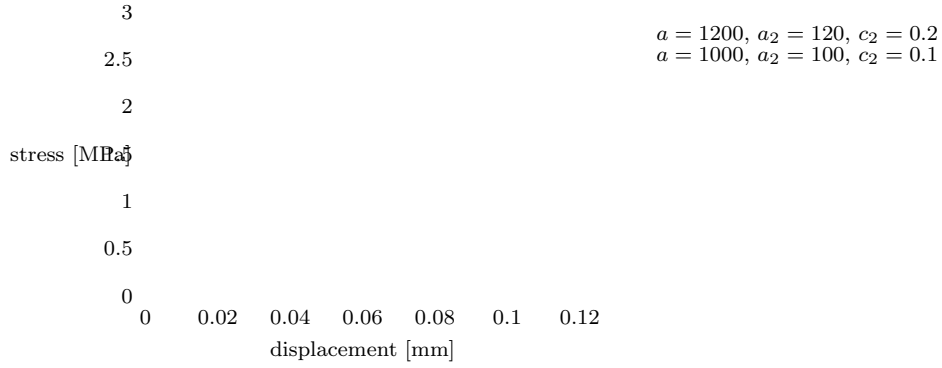

Figure 9: Stress-displacement diagrams for DPM with double-exponential law (61) and parameters $H = 0$, $m = 2$

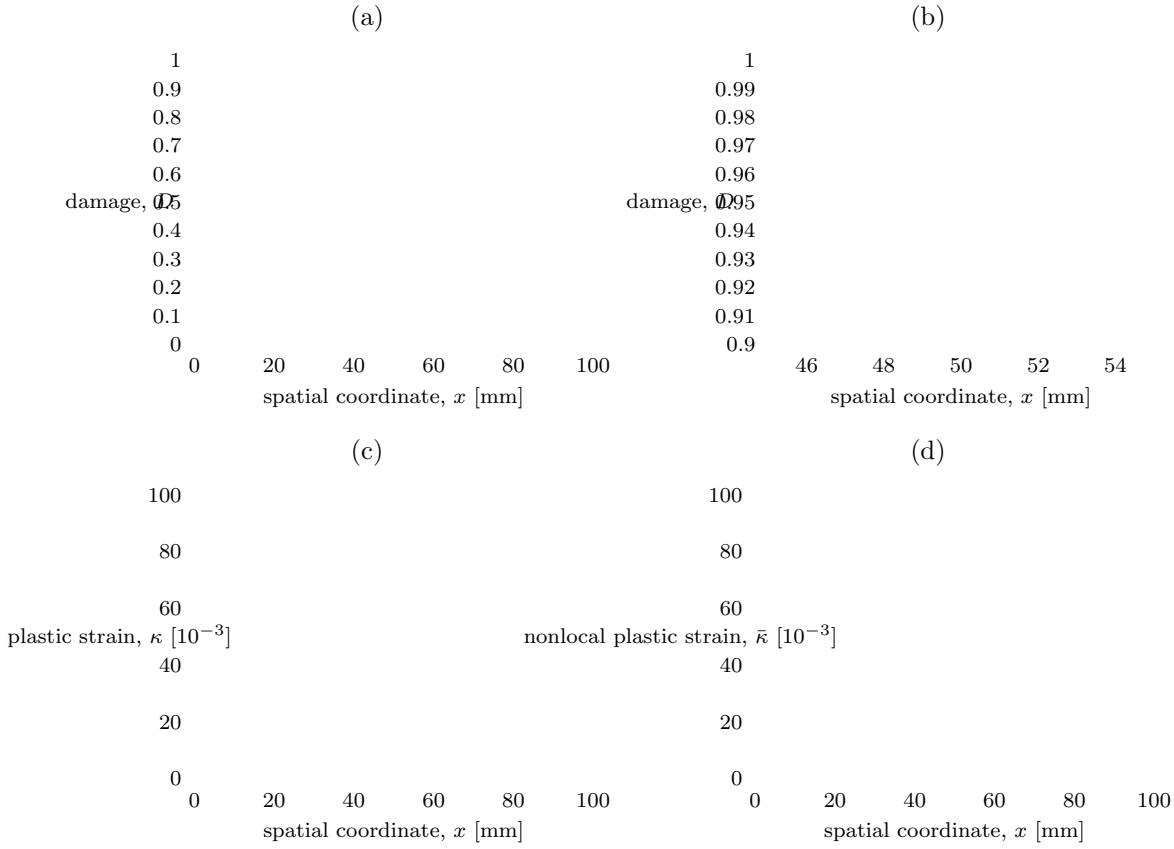

Figure 10: Evolution of the profiles of (a)–(b) damage, (c) local plastic strain and (d) nonlocal plastic strain for DPM with double-exponential law (61) and parameters $H = 0$, $m = 2$

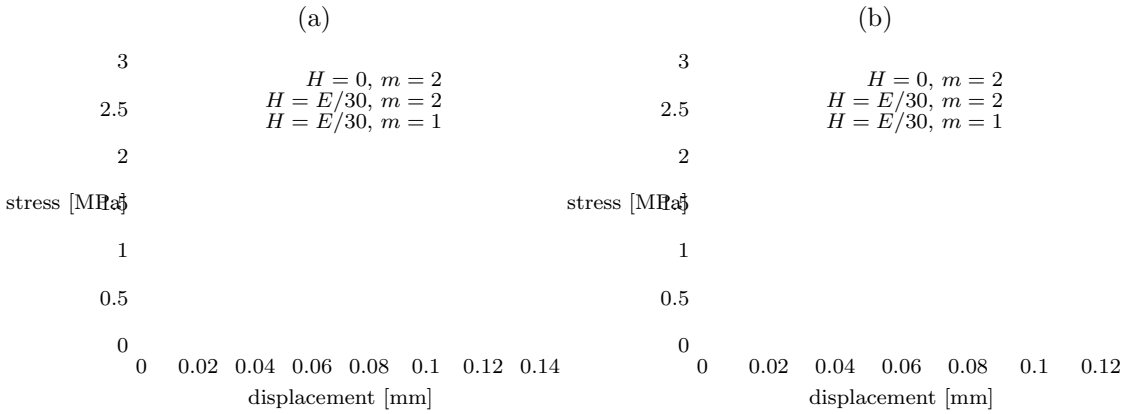

Figure 11: Stress-displacement diagrams for DPM, obtained using (a) double-exponential law (61) with $a = 1200$, $a_2 = 120$ and $c_2 = 0.2$, and (b) double-exponential law (63) with $\varepsilon_f = 0.9333 \cdot 10^{-3}$, $\varepsilon_{f2} = 8.4333 \cdot 10^{-3}$ and $c_2 = 0.2$

also check its extension to the damage-plastic model with a positive hardening modulus H. If we used directly (61) for the damage-plastic model with $H > 0$, the resulting curve would exhibit non-physical bumps; see the dashed and dotted curves in Fig. 11a. Therefore, we need to be more careful.

The objective is to obtain a local softening curve described by the double-exponential function:

$$\sigma_d(\varepsilon) = f_t \left[(1 - c_2) \exp\left(-\frac{\varepsilon - \varepsilon_0}{\varepsilon_f - \varepsilon_0} \right) + c_2 \exp\left(-\frac{\varepsilon - \varepsilon_0}{\varepsilon_{f2} - \varepsilon_0} \right) \right] \tag{62}$$

For the damage-plastic model, this is achieved with

$$\begin{aligned} g_{dp}(\varepsilon_p) &= 1 - \frac{\sigma_d(\varepsilon_p + \sigma_Y(\varepsilon_p)/E)}{\sigma_Y(\varepsilon_p)} = \\ &= 1 - \frac{f_t}{f_t + H\varepsilon_p} \left[(1 - c_2) \exp\left(-\frac{(1 + H/E)\varepsilon_p}{\varepsilon_f - \varepsilon_0} \right) + c_2 \exp\left(-\frac{(1 + H/E)\varepsilon_p}{\varepsilon_{f2} - \varepsilon_0} \right) \right] \end{aligned} \tag{63}$$

For $H = 0$, formula (63) reduces to (61) with $a = 1/(\varepsilon_f - \varepsilon_0)$ and $a_2 = 1/(\varepsilon_{f2} - \varepsilon_0)$, which means that $\varepsilon_f = \varepsilon_0 + 1/a$ and $\varepsilon_{f2} = \varepsilon_0 + 1/a_2$. If the modified formula (63) is used, the bumps become less dramatic but do not completely disappear; see the dashed and dotted curves in Fig. 11b. A potential advantage of the formulation with $H > 0$ is that the damage profiles no longer

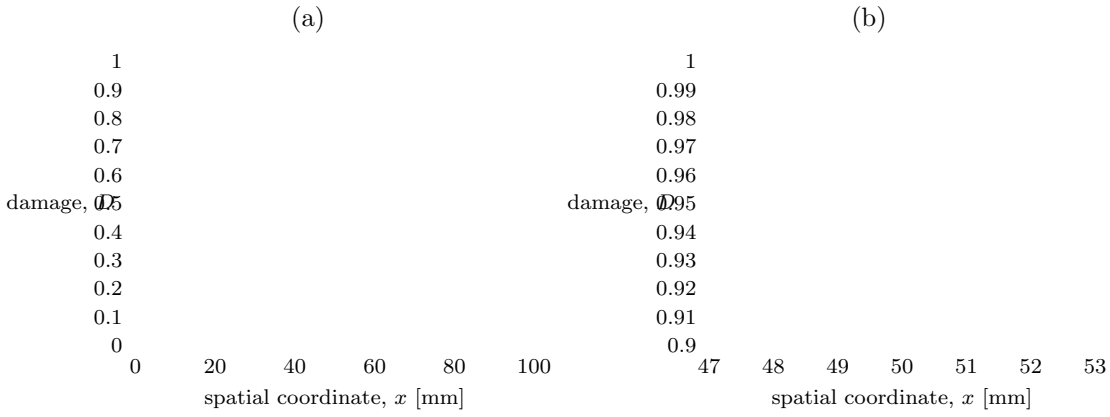

Figure 12: Evolution of damage profiles for DPM with double-exponential law (63) and parameters $H = E/30$, $m = 1$, $\varepsilon_f = 0.9333 \cdot 10^{-3}$, $\varepsilon_{f2} = 8.4333 \cdot 10^{-3}$ and $c_2 = 0.2$

have a central flat part; see Fig. 12a. The active part of the damage zone is shrinking but even at very advanced stages of the damage process contains several elements; see Fig. 12b.

Possible extensions to the pure damage model are analyzed in Appendix C. It is shown that a modified damage law that corresponds to a double-exponential local softening curve would lead to wavy shapes of the stress-displacement diagrams, but a law that corresponds to a properly constructed power-exponential local softening curve can provide, for a specific choice of parameters, a reasonably shaped stress-displacement diagram with a tail.

6. Summary and Concluding Remarks

We have performed a one-dimensional localization analysis of three families of nonlocal softening models suitable for quasi-brittle materials such as concrete, for which the resulting load-displacement curves are supposed to exhibit a long tail similar to an exponential decay. The three considered families of constitutive models were: (i) pure damage models (DM) with no permanent strain, (ii) damage-plastic models (DPM) with permanent strain obtained from plasticity formulated in the effective stress space and with damage driven by the plastic flow, and (iii) models with damage-driven inelastic strains (DMIS), for which

the permanent strains are directly related to damage.

A nonlocal integral (1D) formulation in which the nonlocal interactions are made damage-dependent by using the effective distance defined in (1) has been considered. For this formulation, the computations are found to be mesh-independent, both plastic strain and damage remain localized in a narrow band, and the full damage ($D = 1$) is localized at a single point. The computation of the effective distance $\tilde{r}$ between interacting points is made robust thanks to the proposed scheme (59). An interesting theoretical issue is the precise limiting shape of the damage profile in the uniaxial bar when the displacement tends to infinity and the stress to zero. This point is briefly discussed in Appendix B.

We have focused our attention on the role of permanent strains and on localization properties of formulations that exploit them. We have shown that the dramatic snapback occurring for pure damage models (with no permanent strain at all) can be changed into a long tail (in global stress-displacement response of a bar under uniaxial tension) by accounting for permanent strains. More promising results have been obtained for plasticity-driven permanent strains (DPM) than for damage-driven inelastic strains (DMIS). The present study identifies the formulations that are suitable candidates for extensions of the model to multiple dimensions, in which the evaluation of the effective distance is computationally more demanding.

Acknowledgement:. Financial support received from the Czech Science Foundation (GAČR project No. 17-04150J) is gratefully acknowledged.

References

[1] A.Simone, H. Askes, and L.J. Sluys. Incorrect initiation and propagation of failure in non-local and gradient-enhanced media. *Int. J. Solids Struct.*, 41:351–363, 2004.

[2] A.Simone, G.N. Wells, and L.J. Sluys. From continuous to discontinuous failure in a gradient-enhanced continuum damage model. *Computer Methods in Applied Mechanics and Engineering*, 192:4581–4607, 2003.

[3] Z. P. Bažant. Why continuum damage is nonlocal: micromechanics arguments. *Journal of Engineering Mechanics (ASCE)*, 117:1070–1087, 1990.

[4] Z. P. Bažant. Nonlocal damage theory based on micromechanics of crack interactions. *Journal of Engineering Mechanics (ASCE)*, 120:593–617, 1994.

[5] Z. P. Bažant and M. Jirásek. Damage nonlocality due to microcrack interactions: stastistical determination of crack influence function. In Z. P. Bažant, Z. Bittnar, M. Jirásek, and J. Mazars, editors, *Fracture and Damage in Quasibrittle Structures*, pages 3–17, London UK, 1994. E & FN Spon.

[6] Z. P. Bažant and M. Jirásek. Nonlocal integral formulations of plasticity and damage: Survey of progress. *Journal of Engineering Mechanics (ASCE)*, 128:1119–1149, 2002.

[7] Z. P. Bažant, J. Le, and C. Hoover. Nonlocal boundary layer (nbl) model: overcoming boundary condition problems in strength statistics and fracture analysis of quasibrittle materials. In *FraMCoS-7*, pages 135–143, Korea, 2010.

[8] Z. P. Bažant and G. Pijaudier-Cabot. Nonlocal continuum damage. *Journal of Engineering Mechanics (ASCE)*, 55:287–293, 1988.

[9] T. Belytschko, Y. Krongauz, D. Organ, M. Fleming, and P. Krysl. Meshless methods: An overview and recent developments. *Computer Method in Applied Mechanics and Engineering*, 139:3–47, 1996.

[10] T. Belytschko, Y.Y. Lu, and L. Gu. Crack propagation by element-free galerkin methods. *Engineering Fracture Mechanics*, 51:295–315, 1995.

[11] C. La Borderie. *Phénomènes unilatéraux dans un matériau endommageable.* PhD thesis, Université Paris 6, France, 1991.

[12] G. Borino, B. Failla, and F. Parrinello. A symmetric nonlocal damage theory. *International Journal of Solids and Structure*, 40:3621–3645, 2003.

[13] N. Burlion, F. Gatuingt, G. Pijaudier-Cabot, and L. Daudeville. Compaction and tensile damage in concrete: Constitutive modelling and application to dynamics. *Computer Methods in Applied Mechanics and Engineering*, 183:291–308, 2000.

[14] R. Desmorat. Modèle d'endommagement anisotrope avec forte dissymétrie traction/compression. In *5è journées du Regroupement Francophone pour la Recherche et la Formation sur le Béton (RF2B), 5-6 July, Liège, Belgium*, 2004.

[15] R. Desmorat and F. Gatuingt. Introduction of an internal time in nonlocal integral theories. *Internal report LMT, http://hal.archives-ouvertes.fr/hal-00200898/en/*, 268, 2007.

[16] R. Desmorat, F. Gatuingt, and F. Ragueneau. Nonstandard thermodynamics framework for robust computations with induced anisotropic damage. *International Journal of Damage Mechanics*, 19:53–73, 2010.

[17] Rodrigue Desmorat and Fabrice Gatuingt. Introduction of an internal time in nonlocal integral theories. In *Computational Modelling of Concrete Structures*, pages 121–128, 2010.

[18] Rodrigue Desmorat, Fabrice Gatuingt, and Milan Jirásek. Nonlocal models with damage-dependent interactions motivated by internal time. *Engineering Fracture Mechanics*, 142:255–275, 2015.

[19] P. Feenstra and R. De Borst. A composite plasticity model for concrete. *International Journal of Solids and Structures*, 33:707–730, 1996.

[20] M. Frémond and B. Nedjar. Damage, gradient of damage and principle of virtual power. *International Journal of Solids and Structures*, 33:1083–1103, 1996.

[21] M.G.D. Geers, R. de Borst, W.A.M. Brekelmans, and R.H.J. Peerlings. Strain-based transient gradient damage model for failure analysis. *Computer Methods in Applied Mechanics and Engineering*, 160:133–154, 1998.

[22] C. Giry, F. Dufour, and J. Mazars. Stress-based nonlocal damage model. *International Journal of Solids and Structures*, 48:3431–3443, 2011.

[23] V S Gopalaratnam and S P Shah. Softening response of plain concrete in direct tension. *Journal of the American Concrete Institute*, 82:310–323, 1985.

[24] S. Govindjee, G.J. Kay, and J.C. Simo. Anisotropic modelling and numerical simulation of brittle damage in concrete. *International Journal for Numerical Methods in Engineering*, 38:3611–3633, 1995.

[25] P. Grassl and M. Jirasek. Damage-plastic model for concrete failure. *International Journal of Solids and Structures*, 43:7166–7196, 2006.

[26] Peter Grassl and Milan Jirásek. Plastic model with non-local damage applied to concrete. *International Journal for Numerical and Analytical Methods in Geomechanics*, 30(1):71–90, 2006.

[27] D. Grégoire, L. Rojas-Solano, and G. Pijaudier-Cabot. Failure and size effect for notched and unnotched concrete beams. *Int. J. Numer. Anal. Methods*, 37:1434–1452, 2013.

[28] D. Halm and A. Dragon. An anisotropic model of damage and frictional sliding for brittle materials. *European Journal of Mechanics-A/Solids*, 17:439–460, 1998.

[29] G. Hermann and J. Kestin. On the thermodynamics foundation of a damage theory in elastic solids. In *Cracking and damage*, pages 228–232, 1988.

[30] M. Jirásek, S. Rolshoven, and P. Grassl. Size effect on fracture energy induced by non-locality. *Int. J. Numer. Anal. Methods*, 28:653–670, 2004.

[31] Milan Jirásek and Simon Rolshoven. Comparison of integral-type nonlocal plasticity models for strain-softening materials. *International Journal of Engineering Science*, 41(13-14):1553–1602, 2003.

[32] A. Krayani, G. Pijaudier-Cabot, and F. Dufour. Boundary effect on weight function in nonlocal damage model. *Eng. Fract. Mech.*, 76:2217–2231, 2009.

[33] G. Lebon. *Analyse de l'endommagement des structures de génie civil : techniques de sous-structuration hybride couplées à un modèle d'endommagement anisotrope*. PhD thesis, ENS-Cachan, France, 2011.

[34] J. Lemaitre and J.-L. Chaboche. *Mécanique des matériaux solides*. Dunod, english translation 1990 'Mechanics of Solid Materials' Cambridge University Press, 1985.

[35] M. Matallah and C. La Borderie. Inelasticity-damage-based model for numerical modeling of concrete cracking. *Engineering Fracture Mechanics*, 76:1087–1108, 2009.

[36] J. Mazars, Y. Berthaud, and S. Ramtani. The unilateral behavior of damage concrete. *Engineering Fracture Mechanics*, 76:629–35, 1990.

[37] J. Mazars, S. Ramtani, and Y. Berthaud. An experimental procedure to delocalize tensile failure and to identify unilateral effect of distributed damage. In J. Mazars and Z. P. Bažant, editors, *Cracking and damage: strain localization and size effect*, pages 55–64, London UK, 1989. Elsevier.

[38] G. Meschke, R. Lackner, and A. Mang. An anisotropic elastoplastic-damage model for plain concrete. *International Journal for Numerical Methods in Engineering*, 42:703–727, 1998.

[39] C. Miehe, F. Welschinger, and M. Hofacker. Thermodynamically consistent phase-field models of fracture: Variational principles and multi-field fe implementations. *International Journal for Numerical Methods in Engineering*, 83:1273–1311, 2010.

[40] W. Nechnech, F. Meftah, and J. Reynouard. An elasto-plastic damage model for plain concrete subjected to high temperatures. *Engng Struct*, 24:597–611, 2002.

[41] G. D. Nguyen. A damage model with evolving nonlocal interactions. *International Journal of Solids and Structures*, 48:1544–1559, 2011.

[42] G. Pijaudier-Cabot and Z. P. Bažant. Nonlocal damage theory. *EJ. Eng. Mech. (ASCE)*, 113:1512–1533, 1987.

[43] G. Pijaudier-Cabot and A. Benallal. Strain localization and bifurcation in a nonlocal continuum. *Int. J. Solids Structures*, 30:1761–1775, 1993.

[44] G. Pijaudier-Cabot and F. Dufour. Non local damage model: boundary and evolving boundary effects. *European Journal of Environmental and Civil Engineering*, 14:729–749, 2010.

[45] G. Pijaudier-Cabot, K. Haidar, and J.-F. Dubé. Non-local damage model with evolving internal length. *International journal for numerical and analytical methods in geomechanics*, 28:633–652, 2004.

[46] F. Ragueneau, C. La Borderie, and J. Mazars. Damage model for concrete-like materials coupling cracking and friction, contribution towards structural damping: first uniaxial applications. *Mech. Cohes-Frict. Mater.*, 5:607–26, 2000.

[47] Giuseppe Rastiello, Cédric Giry, Fabrice Gatuingt, and Rodrigue Desmorat. From diffuse damage to strain localization from an Eikonal Non-Local (ENL) Continuum Damage model with evolving internal length. *Computer Methods in Applied Mechanics and Engineering*, 331:650–674, 2018.

[48] L. Rojas-Solano, D. Grégoire, and G. Pijaudier-Cabot. Interaction-based non-local damage model for failure in quasi-brittle materials. *Mechanics Research Communications*, 54:56–62, 2013.

[49] S. Saroukhani, R. Vafadari, and A. Simone. A simplified implementation of a gradient-enhanced damage model with transient length scale effects. *Computational Mechanics*, 51:899–909, 2013.

[50] L Strömberg and M Ristinmaa. FE-formulation of a nonlocal plasticity theory. *Computer Methods in Applied Mechanics and Engineering*, 136:127–144, 1996.

[51] M. Terrien. Emission acoustique et comportement mécanique post-critique d'un béton sollicité en traction. *Bulletin de liaison du LCPC*, 105, 1980.

[52] B. Valentini and G. Hofstetter. Review and enhancement of 3D concrete models for large-scale numerical simulations of concrete structures. *Int. J. Numer. Anal. Meth. Geomech.*, 37:221–246, 2013.

[53] P A Vermeer and R B J Brinkgreve. A new effective non-local strain measure for softening plasticity. In R Chambon, J Desrues, and I Vardoulakis, editors, *Localisation and Bifurcation Theory for Soils and Rocks*, pages 89–100, Rotterdam, 1994. Balkema.

Appendix A: Functions g_{dis} and α_{dis} for Various Versions of DMIS

In this appendix, we present a detailed derivation of the specific form of functions g_{dis} and α_{dis} used by the damage model with inelastic strain. An overview of these functions was provided in Table 1.

Version 1:. It is assumed that the unloading slope is the same as for the DPM with linear hardening of the plastic part. From (28) we obtain

$$\begin{aligned} g_{dis}(\varepsilon) &= g_{dp}(\varepsilon_p(\varepsilon)) = 1 - \frac{f_t}{f_t + H\varepsilon_p(\varepsilon)} \exp\left(-\frac{(1+H/E)\varepsilon_p(\varepsilon)}{\varepsilon_f - \varepsilon_0}\right) = \\ &= 1 - \frac{f_t}{f_t + H(E\varepsilon - f_t)/(E+H)} \exp\left(-\frac{\varepsilon - \varepsilon_0}{\varepsilon_f - \varepsilon_0}\right) = \\ &= 1 - \frac{1}{1 + (E_{ep}/E)(\varepsilon/\varepsilon_0 - 1)} \exp\left(-\frac{\varepsilon - \varepsilon_0}{\varepsilon_f - \varepsilon_0}\right) \end{aligned} \tag{64}$$

where $E_{ep} = EH/(E+H)$ is the elastoplastic modulus of the plastic part of the model.

For a nonzero plastic modulus H, function g_{dis} given by (64) is not invertible in closed form. In fact, this function is not really needed, because the inelastic strain can be evaluated from the damage-driving variable κ_d instead of from the damage D. Equations (18)–(19) can be combined into

$$\varepsilon_p = \alpha_{dis}(g_{dis}(\kappa_d)) \equiv \beta_{dis}(\kappa_d) \tag{65}$$

and function β_{dis} is in general given by the right-hand side of (28), which in the present case leads to

$$\begin{aligned} \beta_{dis}(\varepsilon) &= \varepsilon - \frac{\sigma_d(\varepsilon)}{E[1 - g_{dis}(\varepsilon)]} = \\ &= \varepsilon - \frac{f_t \exp\left(-\dfrac{\varepsilon - \varepsilon_0}{\varepsilon_f - \varepsilon_0}\right)}{\dfrac{E}{1 + (E_{ep}/E)(\varepsilon/\varepsilon_0 - 1)} \exp\left(-\dfrac{\varepsilon - \varepsilon_0}{\varepsilon_f - \varepsilon_0}\right)} = \\ &= \varepsilon - [\varepsilon_0 + (E_{ep}/E)(\varepsilon - \varepsilon_0)] = \frac{E}{E+H}(\varepsilon - \varepsilon_0) \end{aligned} \tag{66}$$

Version 1s:. In the special case with $H = 0$, formula (64) simplifies to

$$g_{dis}(\varepsilon) = 1 - \exp\left(-\frac{\varepsilon - \varepsilon_0}{\varepsilon_f - \varepsilon_0}\right) \tag{67}$$

and becomes invertible in an analytical form. The inverse function is then

$$g_{dis}^{-1}(D) = \varepsilon_0 - (\varepsilon_f - \varepsilon_0)\ln(1-D) \tag{68}$$

In this case, we can apply formula (30) directly and construct an explicit expression for function α_{dis}. After easy manipulations we obtain

$$\alpha_{dis}(D) = g_{dis}^{-1}(D) - \frac{\sigma_d(g_{dis}^{-1}(D))}{E(1-D)} = -(\varepsilon_f - \varepsilon_0)\ln(1-D) \tag{69}$$

Version 2s:. Instead of matching the damage model with inelastic strain to the damage-plastic model, we can match the monotonic stress-strain curve only and postulate the dependence of inelastic strain on damage separately. This approach gives a different type of unloading behavior. Once we postulate the form of function α_{dis}, we can identify function g_{dis} from (27). For instance, if it is assumed that the inelastic strain is proportional to damage, we set

$$\alpha_{dis}(D) = \alpha D \tag{70}$$

where α is a given constant. Equation (27) then becomes

$$[1 - g_{dis}(\varepsilon)]\, E\, [\varepsilon - \alpha g_{dis}(\varepsilon)] = \sigma_d(\varepsilon) \tag{71}$$

which is a quadratic equation with two positive roots. It can be verified that the correct root is the smaller one,

$$g_{dis}(\varepsilon) = \frac{\varepsilon + \alpha - \sqrt{(\varepsilon+\alpha)^2 - 4\alpha[\varepsilon - \sigma_d(\varepsilon)/E]}}{2\alpha} \tag{72}$$

Indeed, at the onset of damage we have $\varepsilon = \varepsilon_0$ and $\sigma_d(\varepsilon) = E\varepsilon$, and formula (72) gives $g_{dis}(\varepsilon_0) = 0$, i.e., zero damage. As ε tends to infinity, $\sigma_d(\varepsilon)$ tends to zero and g_{dis} approaches 1 from below.

Version 2:. For nonlinear functions α_{dis}, the corresponding function g_{dis} usually cannot be constructed analytically, but its values can always be computed numerically. Denoting $g_{dis}(\varepsilon)$ as D, we can rewrite (27) as

$$(1-D)[\varepsilon - \alpha_{dis}(D)] = \frac{\sigma_d(\varepsilon)}{E} \tag{73}$$

or, equivalently, as

$$F(D) \equiv D\alpha_{dis}(D) - \alpha_{dis}(D) - D\varepsilon + \varepsilon - \frac{\sigma_d(\varepsilon)}{E} = 0 \tag{74}$$

This nonlinear equation is solved by the Newton method, starting from the initial approximation $D_0 = 0$, for which $F(D_0) = \varepsilon - \sigma_d(\varepsilon)/E \geq 0$. The derivative of F is given by

$$F'(D) = \alpha_{dis}(D) + D\alpha'_{dis}(D) - \alpha'_{dis}(D) - \varepsilon \tag{75}$$

and so $F'(D_0) = -\alpha'_{dis}(D) - \varepsilon < 0$. The recursive algorithm

$$D_k = D_{k-1} - \frac{F(D_{k-1})}{F'(D_{k-1})}, \qquad k = 1, 2, \ldots \tag{76}$$

should converge to a limit D which represents the value of $g_{dis}(\varepsilon)$. As a specific case, we consider

$$\alpha_{dis}(D) = \alpha D^p \tag{77}$$

where p is a fixed exponent. Then we have

$$F(D) = \alpha D^{p+1} - \alpha D^p - \varepsilon D + \varepsilon - \frac{\sigma_d(\varepsilon)}{E} \tag{78}$$

$$F'(D) = (p+1)\alpha D^p - p\alpha D^{p-1} - \varepsilon \tag{79}$$

Version 3:. One special case in which function α_{dis} is nonlinear but the problem can still be treated analytically is the choice

$$\alpha_{dis}(D) = \alpha \frac{D}{1-D} \tag{80}$$

Equation (73) can then be rewritten as

$$(1-D)\left[\varepsilon - \alpha \frac{D}{1-D}\right] = \frac{\sigma_d(\varepsilon)}{E} \tag{81}$$

which is equivalent to the linear equation

$$(1-D)\varepsilon - \alpha D = \frac{\sigma_d(\varepsilon)}{E} \tag{82}$$

and the solution can be written in closed form as

$$D = \frac{\varepsilon - \sigma_d(\varepsilon)/E}{\varepsilon + \alpha} \equiv g_{dis}(\varepsilon) \tag{83}$$

It is then easy to evaluate the inelastic strain

$$\varepsilon_p = \alpha \frac{D}{1-D} = \alpha \frac{E\varepsilon - \sigma_d(\varepsilon)}{E\alpha + \sigma_d(\varepsilon)} \equiv \beta_{dis}(\varepsilon) \tag{84}$$

Appendix B: Shape of Ultimate Damage Profile

An interesting theoretical issue is the precise shape of the damage profile that is approached in the limit as the displacement tends to infinity and the stress to zero. It is clear that damage at the center of the process zone tends to 1, but is the spatial derivative of damage at this point equal to zero, or is it discontinuous?

Let us place the center of the process zone to the origin ($x = 0$). If the limit damage profile is smooth, the leading term in the expansion of $1 - D(x)$ around the origin is quadratic, and we have

$$D(x) \approx 1 + \frac{1}{2} D''(0) x^2 \tag{85}$$

where $D''(0) < 0$. The integral of $1/\sqrt{1 - D}$ then becomes singular at $x = 0$, because

$$\int \frac{\mathrm{d}x}{\sqrt{1 - D(x)}} \approx \int \frac{\mathrm{d}x}{\sqrt{-D''(0)x^2/2}} = \sqrt{\frac{2}{-D''(0)}} \int \frac{\mathrm{d}x}{|x|} \tag{86}$$

The modified distance between the origin and any other point is then infinite and no interaction takes place across the center of the damage zone.

On the other hand, if the limit damage profile has a kink at the origin, it can be approximated by

$$D(x) \approx 1 + D'(0^+)|x| \tag{87}$$

where $D'(0^+) < 0$, and function $1/\sqrt{1 - D}$ is then integrable:

$$\int \frac{\mathrm{d}x}{\sqrt{1 - D(x)}} \approx \int \frac{\mathrm{d}x}{\sqrt{-D'(0^+)x}} = \frac{1}{\sqrt{-D'(0^+)}} \int \frac{\mathrm{d}x}{\sqrt{|x|}} = \frac{2 \operatorname{sgn} x \sqrt{|x|}}{\sqrt{-D'(0^+)}} \tag{88}$$

In this case, the modified distance is increased but still finite, and points that are sufficiently close can interact even across the center of the damage zone.

Appendix C: Damage Model with Double-Exponential or Power-Exponential Law

In Section 5 it was shown that the tail of the stress-displacement diagram obtained with the damage-plastic model can be extended by reformulating the

damage law. Modifications of the exponential softening law can also improve the shape of the stress-displacement diagrams for the pure damage model. The **double-exponential** stress-strain relation (62) corresponds to the damage function of the pure damage model defined as

$$g_d(\kappa_d) = 1 - \frac{\sigma_d(\kappa_d)}{E\kappa_d} = 1 - \frac{\varepsilon_0}{\kappa_d}\left[(1-c_2)\exp\left(-\frac{\kappa_d-\varepsilon_0}{\varepsilon_f-\varepsilon_0}\right) + c_2\exp\left(-\frac{\kappa_d-\varepsilon_0}{\varepsilon_{f2}-\varepsilon_0}\right)\right] \tag{89}$$

The curves plotted in Fig. 13a have been obtained with parameters $\varepsilon_f = 3\cdot 10^{-4}$ and $\varepsilon_{f2} = 3\cdot 10^{-3}$ and with c_2 ranging from 0 to 0.4. As the value of c_2 is increased, the response becomes less brittle but the softening curves have a wavy shape, which is especially apparent for fine meshes. When ε_f and ε_{f2} are increased, the curves retain the wavy shape; see Fig. 13b.

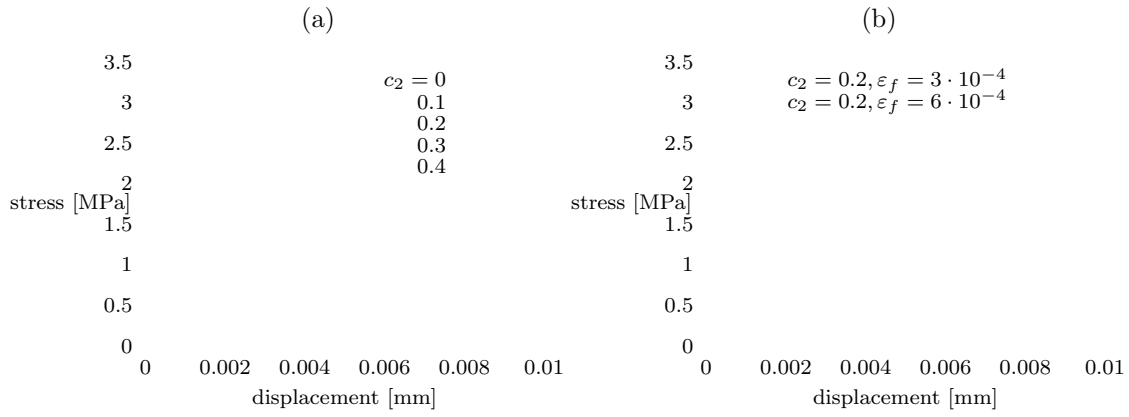

Figure 13: Stress-displacement diagrams for the damage model with the double-exponential law (89): (a) parameters $\varepsilon_f = 3\cdot 10^{-4}$ and $\varepsilon_{f2} = 3\cdot 10^{-3}$ fixed, parameter c_2 varied, (b) parameter $c_2 = 0.2$ fixed, parameters ε_f and $\varepsilon_{f2} = 10\,\varepsilon_f$ varied

The response can be made more ductile not only by adding a slowly decaying exponential, but also by raising the argument of the exponential to a power. The **power-exponential** damage law

$$g_d(\kappa_d) = 1 - \frac{\varepsilon_0}{\kappa_d}\exp\left(-\left(\frac{\kappa_d-\varepsilon_0}{\varepsilon_f-\varepsilon_0}\right)^{m_d}\right) \tag{90}$$

uses an adjustable exponent m_d, and for $m_d = 1$ reduces to (89). As m_d is decreased, the stress-displacement curve changes shape from concave to convex;

see Fig. 14a. A tail is obtained for $m_d = 0.3$ but the response is very brittle right after the peak and the curve exhibits a sharp snapback, only later changing into almost linear softening and a tail. The brittleness right after peak is certainly related to the fact that, for $m_d < 1$, the local stress-strain curve starts at the peak with a vertical slope. This undesirable effect can be removed by reformulating the power-exponential law such that the value of the variable that is raised to m_d is not 0 at the onset of damage. A suitable formula is

$$g_d(\kappa_d) = 1 - \frac{\varepsilon_0}{\kappa_d} \exp\left(-\frac{\kappa_d^{m_d} - \varepsilon_0^{m_d}}{\varepsilon_f^{m_d} - \varepsilon_0^{m_d}} \right) \tag{91}$$

With this damage law, quite a reasonable shape of the stress-displacement curve can be obtained if m_d is set to 0.1; see the solid curve in Fig. 14b.

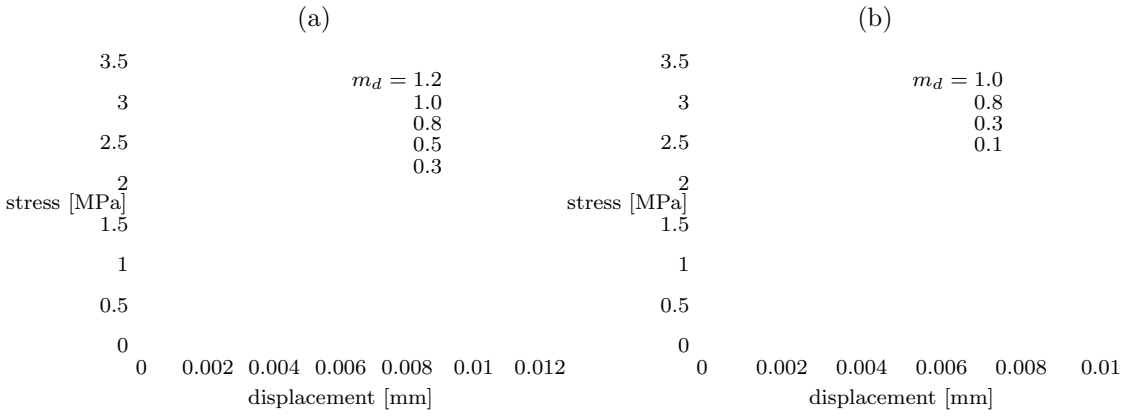

Figure 14: Stress-displacement diagrams for the damage model with a power-exponential law (a) given by (90), (b) given by (91)

Damage profiles corresponding to the last computed step are plotted in Fig. 15 for the model with damage law (90) and in Fig. 16 for the model with damage law (91). In both cases, reduction of exponent m_d leads to more narrow damage profiles that are more rounded around the center of the damage zone (than in the standard case of $m_d = 1$).

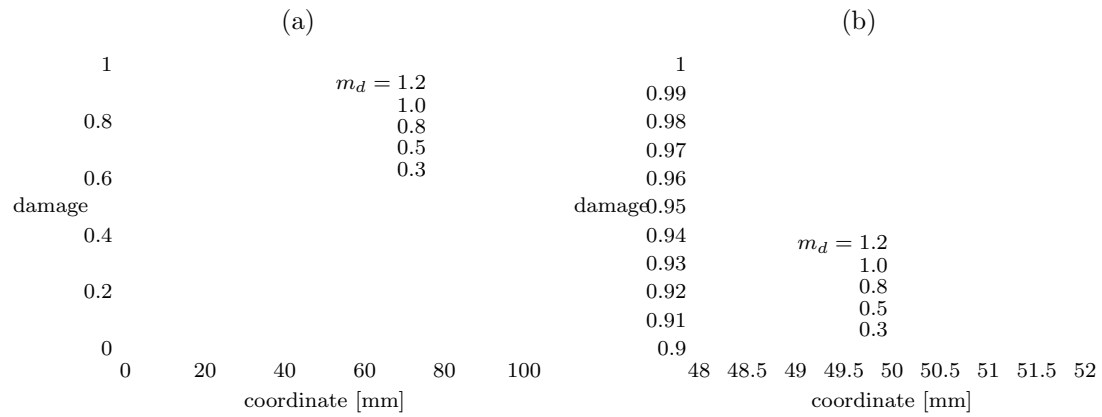

Figure 15: Ultimate damage profiles for the damage model with power-exponential law (90)

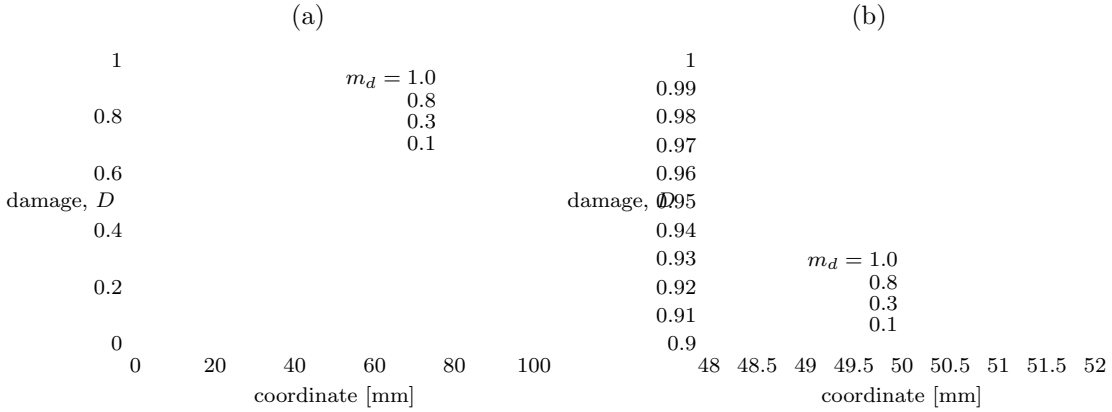

Figure 16: Ultimate damage profiles for the damage model with power-exponential law (91)